Sub-second analysis of locomotor activity in Parkinsonian mice

Daniil Berezhnoi[1,2], Hiba Douja Chehade[1,2], Gabriel Simms[3], Liqiang Chen[1,2], Kishore Kumar S. Narasimhan[4], Shashank M. Dravid[4], and Hong-Yuan Chu[1,2,*]

[1]Department of Pharmacology and Physiology, Georgetown University of Medical Center, Washington DC, 20007, United States

[2]Aligning Science Across Parkinson's (ASAP) Collaborative Research Network, Chevy Chase, MD, 20852, United States

[3]Department of Neurodegenerative Science, Van Andel Institute, Grand Rapids, MI 49503, United States

[4]Department of Psychiatry and Behavioral Sciences, Texas A&M Health Sciences Center, College of Medicine, Texas A&M University, College Station, TX 77845, United States

*Correspondence and Lead contact: Dr. Hong-Yuan Chu, hc948@georgetown.edu

Abstract

The degeneration of midbrain dopamine (DA) neurons disrupts the neural control of natural behavior, such as walking, posture, and gait in Parkinson's disease. While some aspects of motor symptoms can be managed by dopamine replacement therapies, others respond poorly. Recent advancements in machine learning-based technologies offer opportunities to better understand the organizing principles of behavior modules at fine time scales and its dependence on dopaminergic modulation. In the present study, we applied the motion sequencing (MoSeq) platform to study the spontaneous locomotor activities of neurotoxin and genetic mouse models of Parkinsonism as the midbrain DA neurons progressively degenerate. We also evaluated the treatment efficacy of levodopa (L-DOPA) on behavioral modules at fine time scales. We revealed robust changes in the kinematics and usage of the behavioral modules that encode spontaneous locomotor activity. Further analysis demonstrates that fast behavioral modules with higher velocities were more vulnerable to loss of DA and preferentially affected at early stages of Parkinsonism. Last, L-DOPA effectively improved the velocity, but not the usage and transition probability, of behavioral modules in Parkinsonian animals. In conclusion, the hypokinetic phenotypes in Parkinsonism involve the decreased velocities of behavioral modules and their disrupted temporal organization during movement. Moreover, we showed that the therapeutic effect of L-DOPA is mainly mediated by its effect on the velocities of behavior modules at fine time scales. This work documents robust changes in the velocity, usage, and temporal organization of behavioral modules and their responsiveness to dopaminergic treatment under the Parkinsonian state.

Significance Statement

Parkinson's disease is the second largest neurodegenerative disease without a cure. Detection of subtle Parkinsonian signs is critical for disease-modification by applying early interventions. The present work explores the possibility of using machine learning-based approaches for early detection of subtle behavioral changes in Parkinsonian animals and evaluating the therapeutic efficacy of dopaminergic medications.

Key words

Parkinson's disease, dopamine, machine learning, locomotion, motion sequencing, basal ganglia, levodopa

54 **Introduction**

55 Dr. James Parkinson noted Parkinsonian signs by observing individuals on the street and
56 documented the impaired locomotor activities and gait control in patients' daily living [1]. Over
57 decades, the diagnosis of Parkinson's disease (PD) has been primarily conducted in clinical
58 settings, where trained clinicians assess gross motor and cognitive function as well as mental
59 status [2]. However, when and how PD alters patients' behavior in their natural environment
60 remains poorly understood. This is a critical question to address, considering that PD is a chronic
61 and progressive neurological disorder. Detection of motor and nonmotor signs associated with
62 early PD can provide valuable opportunities for effective interventions to alleviate clinical
63 symptoms and even slow down the disease progression. It is established that degeneration of
64 dopaminergic neurons in the substantia nigra pars compacta (SNc) results in hypokinetic
65 symptoms, including akinesia and bradykinesia. Accordingly, restoration of dopamine (DA) levels
66 in the brain by levodopa (L-DOPA) administration can effectively manage hypokinetic symptoms
67 in patients [1]. With emerging machine-learning-based technologies, it becomes possible to use
68 unbiased and data-driven approaches for detailed analysis of motor deficits and the efficacy of
69 dopaminergic medications in PD at fine time scales [3,4]. Such information could reveal new
70 behavioral biomarkers for unbiased PD diagnosis and facilitate the design of effective treatment.

71 Naturalistic motor behavior is generated by orchestrating distinct behavioral modules
72 with different kinematic properties and probability of expression into meaningful actions [5].
73 Recent reports demonstrated that DA levels in the striatum and activities of striatal projection
74 neurons play a critical role in representing and orchestrating behavioral modules into action
75 sequences [6,7]. Building on these observations, decreased striatal DA levels in PD are predicted to

alter the kinematics, the probability of expression, and the organization of behavioral modules into actions, leading to the progressive manifestation of hypokinetic symptoms. In addition, while L-DOPA can effectively improve the motor activity of PD patients, whether L-DOPA restores the basic principles of orchestrating behavioral modules into naturalistic movements remains to be determined.

In the present study, we hypothesized that loss of DA decreases the kinematic measures and frequencies of usage of behavioral modules of naturalistic locomotor activity and that the magnitude of such reduction scales up as the level of striatal DA dampens in PD. We further hypothesized that L-DOPA can restore kinematics and usage of behavioral modules, thereby contributing to its beneficial effects in PD. Here, we employed machine learning-based technologies to perform unsupervised and unbiased segmentation and quantification of spontaneous behavior of two established mouse models of Parkinsonism to test these hypotheses.

90 **Material and Methods**

91 *Animals*

92 Adult C57BL/6 mice (JAX#: 000664, The Jackson Laboratory; RRID: IMSR_JAX:000664) of both
93 sexes at 3-5 months were used for 6-hydroxydopamine (6-OHDA) lesion studies. Mitochondrial
94 transcription factor A (*Tfam*) floxed mice (*Tfam*$^{loxP/loxP}$, JAX#: 026123, The Jackson Laboratory;
95 RRID: IMSR_JAX:026123) and *Dat*-Cre (JAX#: 006660, The Jackson Laboratory; RRID:
96 IMSR_JAX:006660) mice were used to generate the mitoPark mice, as a model of progressive
97 nigrostriatal degeneration [8-10]. Specifically, the double heterozygous mice (*Dat-Cre*$^{Cre/+}$ x
98 *Tfam*$^{loxP/+}$) were crossed with *Tfam*$^{loxP/loxP}$ mice to selectively delete *Tfam* in dopamine neurons,
99 resulting in adult-onset progressive nigrostriatal degeneration and parkinsonian motor deficits.
100 Age-matched littermates with *Tfam*$^{loxP/loxP}$ or *Tfam*$^{loxP/+}$ genotypes were used as controls. Mice
101 were housed up to four animals per cage under a 12/12 h light/dark cycle with access to food
102 and water *ad libitum* in accordance with NIH guidelines for the care and use of animals. All the
103 animal experiments were reviewed and approved by IACUC at Van Andel Institute (AUP# 22-02-
104 006).

105

106 *Stereotaxic surgery*

107 To induce degeneration of nigral DA neurons, we injected 6-OHDA (3–4 mg/ml, 1.0 µl)
108 unilaterally into the medial forebrain bundle (MFB; anteroposterior = −0.7 mm; mediolateral =
109 +1.2 mm; dorsoventral = −4.7 mm) under 2% isoflurane anesthesia over 10 min using a 10-µl
110 syringe (Hamilton). Control animals were injected with HEPES-buffered saline (HBS) in the same
111 location. Desipramine (25 mg/kg) and pargyline (50 mg/kg) were subcutaneously injected 30–

40 min before 6-OHDA injection to reduce damage to the noradrenergic system and enhance the toxicity of 6-OHDA. Mice were allowed to recover after surgery in a heated cage with access to food and water and closely monitored until the behavioral studies.

Behavioral experiments

All behavioral experiments were conducted 3-5 weeks post 6-OHDA or HBS injections. To study progressive changes in the spontaneous behavior during gradual loss of striatal DA, we recorded the open field locomotor behavior of the mitoPark mice 3 ages representing distinct stages of parkinsonism: at 8 weeks with normal striatal DA levels, at 14 weeks with 50% reduction of the striatal DA levels and early motor signs, and at 24 weeks with a nearly complete loss of striatal DA and severe motor deficits [10,11]. A separate cohort of mitoPark mice and littermate controls at >24 weeks received L-DOPA (10 mg/kg, i.p.) and benserazide (15 mg/kg, i.p.) injections to evaluate the treatment efficacy of L-DOPA at sub-second levels. All experiments were performed in a room with dimmed lights. Animals were acclimated to the room and the experimenters prior to recordings. In all experiments, we recorded spontaneous animal behavior for 15-20 min in a square (40x40cm) black-colored box with non-reflective walls and a camera mounted on top (DOI: dx.doi.org/10.17504/protocols.io.e6nvwjxmdlmk/v1). A Microsoft Kinect 2.0 camera was used (30 fps) for recordings from 6-OHDA mice and mitoPark mice, while a FLIR Blackfly S camera (Teledyne Technologies, USA) was used for the mitoPark mice plus L-DOPA experiment. See Key Resource Table for details.

Computational methods

134 For video analysis, we employed the Keypoint-MoSeq tracking algorithms (V. 0.6.2,
135 https://github.com/dattalab/keypoint-moseq, RRID:SCR_025032) [12]. Specifically, 1) Keypoint
136 tracking with ResNet50 network pre-trained on a subset of videos using DeepLabCut pipeline
137 (V.2.3.10, https://github.com/DeepLabCut/DeepLabCut, RRID:SCR_021391), 2) egocentric
138 alignment and cropping, leaving only the postural data, 3) principal component analysis (PCA) to
139 reduce the dimensionality of the resulting time series (5 components for our data), 3)
140 probabilistic modeling fitting autoregressive hidden Markov model (AR-HMM) to the PCA
141 trajectories, 4) fitting full Keypoint-MoSeq model initialized from the AR-HMM, 5) automatic
142 behavioral segmentation and analysis using the motion syllables assigned by the trained model.
143 All the analyses were performed using the provided pipeline in Jupyter Notebooks (V. 7.1.3,
144 https://jupyter.org, RRID:SCR_018315). Training of the model is done through the process of
145 iterative Gibbs sampling while adjusting the Kappa hyperparameter of the model and leaving all
146 other parameters as defaults (Alpha = 5.7, Gamma = 1e3, Max number of states = 1e2) [12].
147 The motion sequencing platform performs probabilistic analysis of the behavior data, and the
148 results depend on the chosen computational model. We fitted our data to multiple models and
149 compared the results before choosing the final model to be applied to all datasets. To select the
150 model, we performed the kappa scanning procedure on our data, training the models with
151 multiple different kappa values and choosing the one that matched our criteria. We used two
152 main criteria to choose a model for further analysis of behavioral videos. The model should (1)
153 match the target duration of the syllable 400 ms (~12 frames at 30 fps) as described previously
154 [5], (2) generate behaviorally meaningful syllables (i.e., consistent behavior modules that an
155 experienced observer can recognize) on the representative grid videos. After the visual

156 screening, the models with inconsistent syllables (e.g., different behavioral modules fall in the
157 same syllable) or too short/long syllables were discarded. Velocity of syllables is calculated by
158 the MoSeq algorithm using the 2d coordinates (x-y) coordinates of the single point (i.e., animal
159 centroid) without including z-axis information. At the same time, MoSeq algorithm assigns a
160 syllable number to each frame. Thus, averaging the differential of the x-y position between all
161 frames assigned to a certain syllable gives the average velocity for that syllable. For conventional
162 locomotor measurement, the velocity is calculated from the x-y coordinates in the MoSeq data
163 frame as the average per the session by dividing the total distance traveled to the time of the
164 session in seconds. For further reference on the exact codes, see the documentation available
165 online (https://keypoint-moseq.readthedocs.io/en/stable/index.html).
166
167 *Immunohistochemical assessment of striatal DA depletion*
168 We used western blot and immunofluorescence staining against tyrosine hydroxylase (TH) in the
169 striatum to assess the level of DA depletion in 6-OHDA mice and the 24 weeks old mitoPark
170 mice, respectively, at the end of this study. 70 µm thick brain sections were prepared using a
171 vibratome (VT1000S; Leica microsystems Inc.). Immunochemical detection of TH was conducted
172 in PBS containing 0.2% Triton X-100 (Fisher Scientific) and 2% normal donkey serum (Sigma-
173 Aldrich). Brain sections were incubated in the primary antibody (mouse anti-TH antibody,
174 1:2000, catalog #MAB318, Sigma-Aldrich, RRID:AB_2313764) for 48 h at 4°C or overnight at
175 room temperature, washed in PBS, and then incubated in the secondary antibody (donkey anti-
176 mouse Alexa Fluor 594, catalog #715-585-150, RRID:AB_2340846) for 90 min at room
177 temperature before washing with PBS. Brain sections were mounted on glass slides using

178 VECTASHIELD antifade mounting medium (catalog #H-1000, Vector Laboratories) and were
179 cover-slipped. TH immunoreactivity in the dorsal striatum and the overlying motor cortex in the
180 same section was imaged using an Olympus BX63F microscope equipped with an Olympus DP80
181 camera or a confocal laser scanning microscope (A1R; Nikon). The intensity of TH
182 immunofluorescence was quantified using ImageJ (NIH). The ratio of TH-immunoreactivity (TH-
183 ir) between the dorsal striatum and the motor cortex was determined to assess the striatal DA
184 depletion in mitoPark mice.

185 Tissue lysate preparation and Immunoblotting. 6-OHDA mice were anesthetized with isoflurane
186 and then decapitated. The brain was removed from the skull and rinsed with ice-cold ACSF to
187 remove any adherent blood. One millimeter (1 mm) coronal sections were taken using brain
188 matrix and the dorsal striatum (dSTR) was punched from the lesioned hemisphere. We used the
189 Allen Brain Atlas: Mouse brain (https://mouse.brain-map.org/static/atlas) as an anatomical
190 reference atlas for punching out the dSTR. The punched tissue was processed for both whole
191 tissue lysate using RIPA buffer (total protein) as well as synaptoneurosomes (fraction containing
192 enriched synaptic components) as previously described [13]. For synaptoneurosomes preparation,
193 dSTR was homogenized in a synaptoneurosome buffer (10 mM HEPES, 1 mM EDTA, 2 mM EGTA,
194 0.5 mM DTT, 0.5 mM PMSF, 50 µg/ml soy-bean trypsin inhibitor, 0.25% of phosphatase inhibitor
195 cocktail 2% and 3%, and 0.25% of protease inhibitor cocktail) and sonicated with 3 pulses (FB50,
196 Fisher Scientific, Pittsburgh, PA, USA). The resulting sample was filtered twice through three
197 layers of a pre-wetted 100 µm pore nylon filter (CMN-0105-D, Small Parts Inc., Logansport, IN,
198 USA) held in a 13 mm diameter filter holder (XX3001200, Milipore, MA, USA). Then the resulting
199 filtrate was filtered once through a pre-wetted 5 µm pore hydrophilic filter (CMN-0005-D, Small

200 Parts Inc.). The filtrate was centrifuged at 1000 × g for 10 min at 4 ºC to obtain the
201 synaptoneurosomes fraction. Isolated synaptoneurosomes were resuspended in
202 synaptoneurosomes buffer containing 0.32 M sucrose, and 1 mM NaHCO3, stored in -80°C until
203 further use. Protein concentration of RIPA lysates and synaptoneurosomes was measured with
204 Pierce™ BCA Protein Assay Kit (Cat# 23227, Thermo Fisher Scientific).
205 Immunoblotting was performed as previously described[13]. Briefly, RIPA lysates and
206 synaptoneurosomes were loaded on 10% sodium dodecyl sulfate gel in equal amounts (50
207 µg/well). The samples were run at 100 volts for 90 min. Gels were transferred to activated
208 (incubation in methanol) polyvinylidene fluoride (PVDF) membrane (GE Healthcare, Piscataway,
209 NJ, USA) at 115 volts for 1 h 45 min. Transfer was blocked with 5% milk in Tris-buffered Saline
210 with 0.1% Tween 20 (TBST) for 1 h at room temperature. The membranes were kept overnight
211 for incubation in primary antibodies including mouse monoclonal anti-tyrosine hydroxylase
212 (1:2000, BioLegend Cat# 818002, RRID: AB_2734573) and mouse monoclonal anti-GAPDH
213 (1:4000, EMD Millipore Cat# MAB374, RRID: AB_2107445) at 4ºC followed by washing with
214 TBST. Blots were incubated with Peroxidase-AffiniPure Goat Anti-Mouse IgG secondary antibody
215 (Jackson ImmunoResearch Labs Cat# 115-035-003, RRID: AB_10015289) for 1 h at room
216 temperature followed by washing with TBST. Blots were incubated with Super-Signal™ West
217 Pico PLUS chemiluminescent substrate (Cat# 34580, ThermoFisher Scientific, Waltham, MA,
218 USA) and developed in a ChemiDoc imaging system (Bio-Rad Laboratories, Inc., USA). The
219 optical density of each sample was analyzed using ImageJ and normalized to GAPDH. Each
220 western blot data point in each group was obtained from a separate animal.
221

Statistical analysis

Data analysis and statistics were performed using Python (Python Programming Language, V.3.9.19, https://www.python.org/downloads/release/python-360, RRID:SCR_008394) and Prism 10 (GraphPad Software, http://www.graphpad.com/,_RRID:SCR_002798). The main parameters of behavioral syllables (e.g., usage and velocity) were calculated for each animal and then averaged within experimental groups. Probability matrices representing the transitions between syllables were generated for each animal and also averaged within groups to represent the differences in behavioral structure. Entropy values were calculated from transition probability matrices as a sum of local entropies per syllable, as reported by [5]. Specifically, Let A denote the estimated transition matrix, so that $A_{ij} = \mathrm{P}[X_{t+1} = j \mid X_t = \mathrm{i}]$ for $i,j = 1,2,\ldots, n$ and all time indices t, and let π denote the steady-state distribution of the Markov chain, so that $\pi_i = \Pr[X_t = \mathrm{i}]$. The entropy rate on the transition matrix was calculated as $\sum_{\mathrm{i,j}} \pi_i A_{ij} \ln A_{ij}$. Data are reported as the mean and standard error of the mean (SEM). Kruskal-Wallis test with post-hoc Dunn's test in the MoSeq package was used to compare the velocity and usage of behavioral syllables across conditions. MoSeq packages corrected raw P values for multiple comparisons using the Benjamini-Hochberg methods, with a false discovery rate (FDR) of 0.05 or less. Mann-Whitney U test was used to compare the statistical significance of the conventional measure of locomotor activity (i.e., velocity) and striatal TH levels between groups, and $\alpha < 0.05$ was considered statistically significant. Details of behavioral analysis can be found at: https://github.com/ChuLab-GU/behavior-analysis

Key Resource Table

RESOURCE TYPE	RESOURCE NAME	SOURCE	IDENTIFIER	NEW/REUSE	ADDITIONAL INFORMATIO
Dataset	Raw behavioral videos in the open field	this paper	10.5281/zenodo.14555868	new	
Dataset	Tabular data used to produce figures	this paper	10.5281/zenodo.14555868	new	
Software/code	Jupyter Notebook 7.1.3	https://jupyter.org/	RRID:SCR_018315	reuse	
Software/code	Python 3.9.19	https://www.python.org	RRID:SCR_008394	reuse	
Software/code	GraphPad Prism 10	http://www.graphpad.com/	RRID:SCR_002798	reuse	
Software/code	FIJI Version 2.10.0	NIH	https://imagej.net/software/fiji/; RRID: SCR_002285	reuse	
Software/code	DeepLabCut pipeline 2.3.10	GitHub	https://github.com/DeepLabCut/DeepLabCut; RRID:SCR_021391	reuse	
Software/code	Keypoint-Moseq code	GitHub	https://github.com/dattalab/keypoint-moseq; RRID:SCR_025032	reuse	
Protocol	Keypoint-Moseq data analysis pipeline	Nature Methods	https://doi.org/10.1038/s41592-024-02318-2	reuse	
Protocol	Stereotaxic surgery protocol	protocols.io	dx.doi.org/10.17504/protocols.io.b9kxr4xn	reuse	
Protocol	Immunohistochemistry protocol	protocols.io	dx.doi.org/10.17504/protocols.io.261ged3j7v47/v2	reuse	
Protocol	Open field assay protocol	protocols.io	https://dx.doi.org/10.17504/protocols.io.e6nvwjxmdlmk/v1	reuse	
Antibody	mouse anti-TH antibody	Sigma-Aldrich	Cat# MAB318, RRID:AB_2313764	reuse	1:2000 dilution
Antibody	donkey anti-mouse Alexa Fluor 488 antibody	Jackson ImmunoResearch	Cat# 715-545-150, RRID:AB_2340846	reuse	1:250 dilution
Antibody	mouse monoclonal anti-tyrosine hydroxylase	BioLegend	Cat# 818002, RRID: AB_2734573	reuse	1:2000 dilution
Antibody	mouse monoclonal anti-GAPDH	MD Millipore	Cat# MAB374, RRID: AB_2107445	reuse	1:4000 dilution
Antibody	Peroxidase-AffiniPure Goat Anti-Mouse IgG secondary antibody	Jackson ImmunoResearch Labs	Cat# 115-035-003, RRID: AB_10015289	reuse	
Experimental model: Organism/strain	C57/BL6 mice	The Jackson Laboratory stock	Strain #000664, RRID: IMSR_JAX:000664	reuse	
Experimental model: Organism/strain	DAT-Cre mice	The Jackson Laboratory stock	Strain #006660, RRID:IMSR_JAX:006660	reuse	
Experimental model: Organism/strain	Tfam flox/flox mice	The Jackson Laboratory stock	Strain #026123, RRID:IMSR_JAX:026123	reuse	
Chemical, peptide, or recombinant protein	L-DOPA	Sigma-Aldrich	catalog #59-92-7	reuse	
Chemical, peptide, or recombinant protein	6-OHDA	HelloBio	catalog #636-00-0	reuse	
Chemical, peptide, or recombinant protein	Triton X-100	Fisher Scientific	catalog #9002-93-1	reuse	
Chemical, peptide, or recombinant protein	Desipramine	Sigma-Aldrich	catalog #58-28-6	reuse	
Chemical, peptide, or recombinant protein	Vectashield medium	Vector Laboratories	catalog #H-1000	reuse	
Chemical, peptide, or recombinant protein	Pargyline	Sigma-Aldrich	catalog #306-07-0	reuse	
Other	Microsoft Kinect 2.0 camera	https://www.newegg.com/	https://www.newegg.com/p/2NG-004G-00002	reuse	
Other	FLIR Blackfly S camera	https://www.edmundoptics.com/	catalog #11-509	reuse	
Other	Leica VT1000S vibratome	Leica Microsystems Inc.	catalog #14047235613	reuse	
Other	Confocal microscope Nikon A1R	Nikon	catalog #A1R HD25_2CE-SCNH-5	reuse	

247 **Results**

248 **Loss of DA alters the velocity and usage of behavioral modules**

249 First, we employed mice with 6-hydroxydopamine (6-OHDA) lesions as a model of nigrostriatal
250 degeneration, which is known to recapitulate behavioral phenotypes and pathophysiological
251 features of human PD and has been widely used for preclinical PD research [14-19]. To model an
252 advanced Parkinsonian state with nearly complete DA depletion, we injected 6-OHDA into the
253 MFB to induce degeneration of the nigrostriatal pathway and nearly complete striatal DA
254 depletion (**Figure 1A, B**) [15,17,20]. Three weeks post-surgery, locomotor activities of 6-OHDA- and
255 vehicle-injected mice (i.e., 6-OHDA mice and controls, respectively) were recorded for 20 min in
256 an open field arena. Analysis of conventional locomotor measures demonstrates that 6-OHDA
257 mice showed a significant reduction of general motor activity relative to controls (e.g., velocity,
258 control = 8.9±0.6 cm/sec, n = 6 mice; 6-OHDA = 5.5±0.2 cm/sec, n = 7 mice; $P < 0.001$). These
259 results confirm the severe Parkinsonian motor deficits following the degeneration of the
260 dopaminergic nigrostriatal pathway.

261 **Fig 1 here**

262 **Figure 1. Loss of DA alters the velocity and usage of behavioral modules of 6-OHDA mice. A)** Western blotting
263 analysis of synaptoneurosome and RIPA lysate TH protein from the dorsal striatum of control and 6-OHDA mice. A
264 significant reduction of striatal TH protein as seen in both synaptoneurosome ($p = 0.0023$, n = 3 mice/group,
265 Welch's t test) and RIPA lysate ($p = 0.03$, n = 3mice/group, Welch's t test). **C)** Representative behavioral syllables
266 identified by MoSeq. **D-E)** Syllable velocity (D) and usage (E) of 6-OHDA mice and controls ranked by velocities for
267 visualization. Arrows indicated the representative syllables in (C). Asterisks indicate syllables showing statistical
268 significance in either the syllable velocities (D) or usage (E) between 6-OHDA mice and controls. See Table 1 for the
269 source data. **F-G**) Differences in syllable velocities (Δvelocity, D) or usage (Δusage, E) between controls and 6-OHDA

270 mice were plotted against the syllable velocities in controls. **H**) Transition graphs representing the changes in
271 behavioral structure as an increase (red) or decrease (blue) in the probability of transition between numbered
272 syllables in 6-OHDA mice relative to controls. **I-J**) Representative plots showing the temporal organization of
273 spontaneous behavior in controls (I) and 6-OHDA mice (J). Different colors represent distinct behavioral syllables.
274 Only six 6-OHDA mice were shown in the representative plot. **K**) Summarized bar plot showing the reduced
275 transition frequency of syllables in 6-OHDA mice relative to controls (control = 1.8±0.03, n = 6 mice; 6-OHDA =
276 1.48±0.07, n = 7 mice, P = 0.008, Mann-Whitney U test). **L**) Summarized bar plot showing a nonsignificant change in
277 the transition entropy of syllables in 6-OHDA mice relative to controls (control = 5.78±0.04, n = 6 mice; 6-OHDA =
278 5.63±0.06, n = 7 mice, P = 0.1, Mann-Whitney U test).

279 Next, we employed the motion sequencing (i.e., MoSeq) approach to interrogate the
280 locomotor activity of Parkinsonian mice at fine timescales. MoSeq automatically identifies
281 behavioral modules at sub-second levels (i.e., syllables) and determines the probability of their
282 usage in locomotor activities [3-7,12,21]. MoSeq recognized morphologically distinct sub-second
283 behavioral syllables with comparable mean durations of 588±5.7 ms for controls and 538±6.3
284 for 6-OHDA mice. Among all the identified behavioral modules, 21 syllables were expressed
285 more than 0.5% of the time (see examples in **Figure 1C**). Each syllable could be described as a
286 behavior module by a human observer, including various pauses (e.g., syllable 19), freezing (i.e.,
287 no change in body location for 1 sec or more, syllable 18), run (e.g., syllable 5 and 14), grooming
288 (e.g., syllable 24), rearing, and turns. Although unilateral turnings are behavioral features of
289 mice with 6-OHDA lesion, they were not identified as a single syllable by Moseq. This might be
290 because spontaneous unilateral turnings in an open field arena usually take longer than a
291 second. In the rest of the study, we focused on the 21 most frequently used and meaningful
292 behavior modules to characterize Parkinsonian phenotypes in mice at the sub-second level.

293 For the purpose of visualization, we ranked syllables based on their velocities, ranging
294 from faster run-like syllables to slower freezing-like syllables (**Figure 1C-D**). We found a
295 significant decrease in the velocities of faster syllables of 6-OHDA mice relative to controls (e.g.,
296 the velocity of syllable# 14 [i.e., run], controls = 17.2±0.36 cm/sec, n = 6 mice; 6-OHDA =
297 9.2±0.6 cm/sec, n = 7 mice, $P < 0.0001$, **Figure 1D**). In contrast, the velocities of most slower
298 syllables (e.g., pause and freezing) were not altered between groups (e.g., the velocities of
299 syllable#18 [i.e., freezing], controls = 3.19±0.045 cm/sec, 6-OHDA mice = 3.14±0.019 cm/sec;
300 the velocities of syllable#19 [i.e., pause], controls = 7.5±1.1 cm/sec, n =6 mice; 6-OHDA mice =
301 5.76±0.72 cm/sec, n = 7 mice, $P > 0.05$, **Figure 1D**). Next, we analyzed the frequency of
302 expression (i.e., the usage) of behavioral syllables in 6-OHDA mice and controls. There were
303 significant decreases in the usage of faster syllables and increases in the usage of slower
304 syllables in the 6-OHDA mice relative to controls (**Figure 1E**). For example, 6-OHDA mice used
305 the faster syllable#14 significantly less than controls (controls = 0.013±0.002, n = 6 mice; 6-
306 OHDA = 0.003±0.0008, n = 7 mice; $P < 0.0001$). In contrast, 6-OHDA mice expressed the slower
307 syllable#18 more frequently than controls (controls = 0.04±0.0065, n = 6 mice; 6-OHDA =
308 0.09±0.008, n = 7 mice, $P = 0.002$).

309 Further, we tested the hypothesis that loss of DA has stronger effects on faster syllables.
310 To do this, we assessed the correlation between the group differences in the velocities and
311 usages [i.e., Δvelocities$_{(control\text{-}6\text{-}OHDA)}$ and Δusage$_{(control\text{-}6\text{-}OHDA)}$, respectively) against the syllable
312 velocities of controls (**Figure 1F, G**). Linear regression analysis showed a strong correlation
313 between the Δvelocities and syllable velocities in controls ($R^2 = 0.87$, $P < 0.0001$, **Figure 1F**).

314 Similarly, a statistically significant linear relationship was detected between Δusage and syllable
315 velocities in controls (R^2 = 0.27, P = 0. 0165, **Figure 1G**).
316 Together, these results suggest that while the kinematics and usage of behavior modules
317 are altered following the loss of DA, the changes neither uniform nor unidirectional. Specifically,
318 the nigrostriatal dopaminergic degeneration preferentially decreases the kinematics of faster
319 behavioral modules and disrupts the usage of various behavioral modules, resulting in
320 Parkinsonian motor deficits.
321
322 **Loss of DA alters the transition probability of behavioral modules**
323 Disrupted usage of behavioral modules is expected to alter the temporal organization of
324 syllables into actions. Indeed, the transition matrix showed that the transition probabilities
325 were up- and down-regulated among subsets behavioral syllables (**Figure 1H**). Moreover, we
326 plotted the temporal organization of behavioral syllables in controls and 6-OHDA mice to further
327 assess the patterns of behavioral module expression and transition. Relative to controls, 6-
328 OHDA mice exhibited prolonged expression of a subgroup of syllables, leading to decreases in
329 syllable transitions (**Figure 1I, J**). We employed entropy (i.e., a measure of disorder level) and
330 the frequency of transitions to quantify the temporal organization of behavioral syllables (**Figure**
331 **1K, L**) [5]. Quantitative analysis confirmed less frequent syllable transitions in 6-OHDA mice than
332 in controls. Specifically, the number of syllable transitions decreased significantly in 6-OHDA
333 mice relative to controls (**Figure 1K**). However, the difference in entropy did not reach statistical
334 significance between 6-OHDA mice and controls (**Figure 1L**). These data indicate that
335 Parkinsonian animals exhibited fewer behavior module transitions and distinct pattern of

336 organizing rules of syllables during naturalistic behavior. This is consistent with a recent study
337 reporting that elevated DA levels in the striatum increase the variabilities of behavioral
338 modules, making them less predictable during naturalistic motor activities [7].

339 Taken together, the above data suggest that hypokinetic symptoms in the Parkinsonian
340 state involve the abnormal sub-second architecture of locomotor behavior, as reflected by 1)
341 the reduced velocities of subsets of syllables, (2) disrupted usage and altered temporal
342 organization of behavioral syllables, and 3) decreased frequency of syllable transitions during
343 spontaneous locomotion activities.

344 **Fig 2 here**

345 **Figure 2. Time course of velocity changes of behavioral modules in mitoPark mice. A)** mitoPark mice showed a
346 complete loss of striatal TH immunoreactivity at 24 weeks (control = 8.5±0.98, n = 8; mitoPark = 1.1±0.12, n = 7, $p <$
347 0.0001). **B)** mitoPark mice exhibited a progressive reduction in general locomotory activity relative to littermate
348 controls Locomotion speed: At 8 weeks, controls = 8.85±0.34 cm/sec, n = 11 mice, mitoPark = 9.04±0.33 cm/sec, n
349 = 11 mice, P = 0.3; At 14 weeks, controls = 9.21±0.23 cm/sec, n = 8 mice, mitoPark = 6.88±0.34 cm/sec, n = 8 mice,
350 P = 0.0002; At 24 weeks, controls = 8.03±0.22 cm/sec, n = 7 mice, mitoPark = 4.53±0.15 cm/sec, n = 9 mice, P =
351 0.0002. **C**) Representative syllables showing significant changes in syllable velocities at early and late motor stages
352 in mitoPark mice relative to controls. **D-F**) Plots showing progressive reduction of syllable velocities in mitoPark
353 mice relative to age-matched littermate controls at 8-, 14-, and 24-weeks. Arrows indicate the representative
354 syllables shown in (B). Asterisks showing the syllables with statistically significant changes between mitoPark mice
355 and littermate controls. See Table 2 for details. **G-H**) Differences in syllable velocities (Δvelocity) between mitoPark
356 mice and littermate controls were plotted against the syllable velocities in controls.

357

358 **Time course of velocity changes of behavioral modules in progressive Parkinsonism**

359 PD is a chronic and progressive neurodegenerative disease that affects various aspects of motor
360 control and body movements. Next, we depicted how the observed changes in behavior
361 modules emerge from the early to late stages of Parkinsonism. To address this question, we
362 utilized the mitoPark mice as a model of progressive degeneration of the nigrostriatal
363 dopaminergic pathway (**Figure 2A**) [8-10,22]. Based on the evidence in the literature, we identified
364 the following age groups of mitoPark mice to study: baseline state at 8 weeks with normal
365 motor function, early motor stage at 14 weeks, and advanced motor stage at 24 weeks [11].
366 Spontaneous open-field locomotor activities of mitoPark mice and littermate controls were
367 recorded at 8, 14, and 24 weeks of age. Analysis of locomotory activity using conventional
368 measures confirmed that mitoPark mice showed normal general motor activity at 8 weeks, but
369 exhibited gradual decreases in movement speed from 14 to 24 weeks of age (**Figure 2B**). This
370 time course of Parkinsonism development in mitoPark mice is consistent with previous reports
371 [8-10,22].

372 MoSeq was used to analyze the locomotor activities of mitoPark mice to reveal potential
373 changes in kinematics, usage, and organization of behavior syllables at different age groups.
374 MoSeq identified 99 behavioral syllables expressed by mitoPark mice and littermate controls
375 with a mean duration of 603.5±6.1 ms. 22 out of 99 syllables were used more than 0.5% of the
376 time by animals of both genotypes. Thus, we focused on these 22 most enriched behavioral
377 syllables to characterize the evolvement of the usage and sequence of behavior modules as the
378 nigrostriatal dopaminergic pathway degenerates progressively (**Figure 2C**).

379 Consistent with the conventional analysis of locomotor activities (**Figure 2B**), mitoPark
380 mice showed no difference in the velocity of various syllables relative to littermate controls at 8

381 weeks of age (**Figure 2D**). At the early motor stage (i.e., 14 weeks), 10 out of 22 syllables
382 showed reduced velocities in mitoPark mice relative to littermate controls (**Figure 2C, E**). At the
383 advanced motor stage (i.e., 24 weeks), 14 out of 22 syllables showed decreased velocities in
384 mitoPark mice relative to littermate controls (**Figure 2C, F**). Moreover, the syllables with higher
385 velocities (e.g., run-like modules, **Figure 2C**) showed earlier decreases in the velocity, and the
386 magnitude of such changes scaled up from the early to the advanced motor stages. For
387 example, the velocity of the run-like syllable 21 showed 20% reduction at 14 weeks (controls =
388 16.2±0.59 cm/sec and mitoPark = 12.98±0.67 cm/sec, n = 8 mice/group, P = 0.014); and 38%
389 reduction at 24 weeks (controls = 16.7±0.8 cm/sec, n = 7 mice; mitoPark = 10.45±1.21 cm/sec, n
390 = 8 mice; P = 0.001). As the nigrostriatal dopaminergic pathway degenerated, additional
391 syllables significantly reduced their velocities from the early motor stage to the advanced stages
392 (**Figure 2C, E, F**). Most syllables showing significant changes in velocities at 24 weeks were those
393 involving whole body movements (**Figure 2C, F**), including various turns (e.g., syllable 7),
394 grooming (e.g., syllable 4),

395 Similar to the mice with 6-OHDA lesion, simple linear regression analysis showed a
396 strong correlation between the Δvelocity (i.e., controls minus mitoPark mice) and syllable
397 velocities of respective controls at 14 and 24 weeks (regression coefficient, 14 weeks = 0.22, P <
398 0.0001; 24 weeks = 0.39, p < 0.0001) (**Figure 2G-H**). Thus, hypokinetic parkinsonian motor
399 deficits could be partially explained by the progressive reduction of the kinematics of a subset
400 of faster behavioral modules as the nigral DA neurons progressively degenerate.

401

402 **Time course of usage changes of behavioral modules in progressive Parkinsonism**

403 **Fig 3 here**

404 **Figure 3. Time course of usage changes of behavioral modules in progressive Parkinsonism. A)** Representative
405 syllables showing changes in usage in mitoPark relative to littermate controls. **B-D**) Plots of syllable usage between
406 mitoPark mice and littermate controls at 8-, 14-, and 24 weeks. Arrows indicate the representative syllables shown
407 in (A). Asterisks indicate syllables showing statistically significant changes in the usage across time. **E**)
408 Representative plots showing the temporal organization of spontaneous behavior in controls (upper) and mitoPark
409 mice (bottom) at 24 weeks. **F**) Transition graphs representing the changes in behavioral structure as an increase
410 (red) or decrease (blue) in the probability of transition between numbered syllables in mitoPark mice relative to
411 controls. **G-H**) Summarized graphs showing reduced transition entropy (At 8 weeks, control = 5.32±0.03, n = 11,
412 mitoPark = 5.28±0.05, n = 11, P = 0.56; At 14 weeks control = 5.22±0.06, n = 8, mitoPark = 5.23±0.06, n=8, P = 0.88;
413 At 24 weeks control = 5.45±0.03, n = 7, mitoPark = 5.17±0.05, n = 9, P =0.0007; Mann-Whitney U test) and
414 transition frequency (H, At 8 weeks control = 1.59±0.03, n = 11, mitoPark = 1.57±0.03, n = 11, P =0.4; At 14 weeks
415 control = 1.56±0.04, n = 8, mitoPark = 1.48±0.05, n = 8, P = 0.38; At 24 weeks control = 1.76±0.06, n = 7, mitoPark =
416 0.85±0.05, n = 9, P = 0.0002; Mann-Whitney U test) of behavioral modules in mitoPark mice at 24 weeks, but not at
417 earlier stages, relative to littermate controls.

418

419 When the syllable usage was compared between groups, mitoPark mice gradually
420 showed a subset of differently expressed behavioral modules relative to controls (**Figure 3A-D**).
421 Specifically, the usage of behavioral modules was comparable between controls and mitoPark
422 mice at 8 weeks, except for a transient and slight increase in the usage of syllable 16 by
423 mitoPark mice (**Figure 3B**). At 14 weeks, mitoPark mice showed three additional differently
424 expressed behavioral modules relative to littermate controls, including an upregulation of a
425 freezing-like module (i.e., syllable 9) and a downregulation of a run-like module (e.g., syllable 1).
426 At 24 weeks, mitoPark mice showed 13 differently expressed behavioral modules, which further

427 diverged from the pattern of syllable usage in controls (**Figure 3D**). These changes in syllable
428 usage were not unidirectional, including upregulation of pause-like behavior (e.g., syllable 18) as
429 well as downregulations of faster modules (e.g., syllable 14: run) and the syllables involving
430 large-amplitude whole body movements (e.g., syllable 6: turns). These data suggest that the
431 gradual loss of DA altered the usage of syllables multi-directionally, not uniformly, depending on
432 their distinct roles in organizing naturalistic behavior.

433 In addition to the emergence of differently expressed behavioral modules over time, the
434 difference in their usage was scaled up from the early to late stages of Parkinsonism. For
435 example, the magnitude of reduction in the usage of fast syllables 1 and 3 of mitoPark mice
436 relative to controls continued decreasing from 14 weeks to 24 weeks (see Table 2 for details).
437 These observations are consistent with the concept that striatal neuronal activities modulate
438 the vigor of movement that is closely linked to rapid DA release in the striatum [7,23].

439

440 **Time course of temporal organization of behavioral modules in progressive Parkinsonism**

441 Next, we studied how progressive loss of DA affects the temporal organization of spontaneous
442 locomotor activity. Plotting the expression of distinct syllables against time revealed that control
443 mice exhibited dynamic and frequent transitions among behavior modules in locomotion
444 (**Figure 3E**). However, such dynamic syllable transitions became less frequent in mitoPark mice,
445 particularly at 24 weeks of age (**Figure 3E, G, H**). A few syllables, including syllable 0 (rearing),
446 syllable 8 (grooming), and syllable 11 (slow walk) occupied long periods of time in mitoPark
447 mice (**Figure 3E**). This conclusion was further supported by emerging differences in syllable
448 transition probabilities between controls and mitoPark mice across ages (**Figure 3F**), manifesting

449 as upregulated transition probability between a subset of syllables but downregulated transition
450 probability between other syllables. The above data suggest that the naturalistic behavior of
451 progressive mitoPark mice becomes more stereotypical and predictable as midbrain DA neurons
452 progressively degenerate, recapitulating key findings from the 6-OHDA mice with complete DA
453 depletion.
454

455 **Fig.4 here**

456 **Figure 4. L-DOPA partially restores behavioral modules of mitoPark mice. A)** Representative syllables showing
457 significant changes in either velocities or usage between mitoPark mice and littermate controls. This subset of
458 syllables was selected to study L-DOPA's treatment efficacy. **B**) Summarized graph showing L-DOPA rescued the
459 reduced velocity of behavioral syllables in mitoPark mice. **C-D**) Summarized graphs showing that L-DOPA affects the
460 usage of neither the downregulated nor the upregulated behavioral syllables in mitoPark mice relative to the
461 control. **E**) Representative plots showing the temporal organization of spontaneous behavior in controls (upper),
462 mitoPark mice (middle), and mitoPark mice treated with L-DOPA (bottom) at 24 weeks. Different colors represent
463 distinct behavior syllables. **F**) Transition graphs representing the changes in behavioral structure as an increase
464 (red) or decrease (blue) in the probability of transition between numbered syllables. **G**) Summarized graphs
465 showing reduced transition frequency (G, control = 2.27±0.23, n = 9; mitoPark = 0.96±0.14, n = 9, P = 0.0002 vs.
466 control; mitoPark + L-DOPA = 1.07±0.05, n = 9, P > 0.05 vs. mitoPark) and transition frequency (H, control =
467 5.42±0.12, n = 9; mitoPark = 4.98±0.096, n = 9, P = 0.05 vs. control; mitoPark + L-DOPA = 4.76±0.19, n = 9, P > 0.05
468 vs. mitoPark) of behavioral modules in mitoPark mice at 24 weeks, which was not rescued by L-DOPA treatment.
469

470 **L-DOPA effectively increases the velocity of behavioral modules in Parkinsonism but exerts a**
471 **negligible effect on their usage.**

472 The mitoPark mice with advanced Parkinsonism are responsive to the L-DOPA administration [9].
473 Next, we determined if L-DOPA can rescue the altered kinematics and usages of behavioral
474 modules of mitoPark mice at 24 weeks. We intraperitoneally (i.p.) injected L-DOPA (10 mg/kg)
475 and saline to mitoPark mice and age-matched controls, followed by monitoring their locomotor
476 activities in an open field arena for 20 min. Analysis of conventional measurements of
477 locomotor activity showed that L-DOPA administration effectively alleviated parkinsonian
478 hypokinetic deficits of mitoPark mice (speed of locomotion, saline-injected control = 10.3±1.2
479 cm/sec, n = 9 mice; saline-injected mitoPark = 4.0±0.36 cm/sec, n = 9 mice, p = 0.004 vs saline-
480 injected controls; mitoPark with L-DOPA = 14.4.9±2.97 cm/sec, n = 9 mice, P = 0.003 vs saline-
481 injected mitoPark mice).

482 MoSeq identified various behavioral modules showing altered velocity and usage among
483 groups. To determine the beneficial effects of L-DOPA, we identified a subset of behavior
484 modules showing significant changes in their velocity and usage between saline-injected
485 controls and mitoPark mice. Specifically, a group of fast behavioral modules, including run- and
486 turn-like behaviors, showed decreased velocities between saline-injected mitoPark and saline-
487 injected controls (**Figure 4A**). The velocities of most of these behavioral modules were
488 significantly increased by L-DOPA administration. For example, the velocities of syllable 1 were
489 10.3±1.37 cm/sec in saline-injected controls (n= 5), 4.9±0.27 cm/sec in saline-injected mitoPark
490 mice (n = 9), and 9.44±1.29 cm/sec in mitoPark with L-DOPA (n = 9) (saline-injected controls
491 versus saline-injected mitoPark, P < 0.001; saline-injected mitoPark versus mitoPark with L-
492 DOPA, P = 0.009, **Figure 4B**, see Table 3 for details).

493 Moreover, mitoPark mice exhibited both down- and up-regulated usage of behavioral
494 modules. Surprisingly, L-DOPA treatment failed to restore the usage of downregulated modules
495 in mitoPark mice (**Figure 4C**). When it comes to the upregulated behavior modules, the L-DOPA
496 did not restore their frequency of expression either (**Figure 4D**). The above data suggest that L-
497 DOPA administration increased the velocities of behavioral modules during spontaneous
498 locomotory activity but had little effect on their usage in the Parkinsonian state.

499 Given the negligible effect of L-DOPA on syllable usage of the advanced mitoPark mice,
500 we predicted that L-DOPA does not affect the transition probabilities and temporal organization
501 of behavior modules in the Parkinsonian state. As predicted, we found that L-DOPA
502 administration did not rescue the reduced behavior module transitions in mitoPark mice (**Figure**
503 **4E-H**). Specifically, neither the reduced transition frequencies (**Figure 4G**) nor the entropy
504 (**Figure 4H**) in mitoPark mice was improved by L-DOPA administration. The above data suggest
505 that the disrupted syllable usage and their temporal organization in Parkinsonian mice were not
506 responsive to dopaminergic medication.

507 Altogether, the above results suggest that acute L-DOPA significantly improves the motor
508 function of Parkinsonian mice and that its beneficial effect was mediated mainly by increasing
509 the velocities of behavioral modules. L-DOPA administration produced little effect on the usage
510 of behavior modules and their transitions during naturalistic locomotor behavior.

511

512 **Discussion**

513 In the present study, we employed an unbiased and unsupervised approach to quantify the
514 naturalistic locomotor behavior under Parkinsonian state. Using 6-OHDA mice with complete DA
515 depletion, we demonstrate that complete loss of DA decreases the syllable velocities, disrupts
516 the pattern of syllable usage, and reduces the transition probabilities among behavior modules
517 (**Figure 1**). Correlation analysis further showed a stronger effect of DA depletion on the velocity
518 and usage of behavioral modules with higher velocities (**Figure 1**). These observations are
519 further confirmed and validated by using the mitoPark mice, a genetic and progressive model of
520 Parkinsonism (**Figures 2 and 3**). The beneficial effects of L-DOPA on motor symptoms in PD have
521 been well-established for decades. Therefore, we further analyzed the effects of L-DOPA on
522 behavioral modules at the sub-second time scale. We demonstrate that L-DOPA effectively
523 restored the decreased velocity but had a negligible effect on the disrupted usage of behavioral
524 syllables of mitoPark mice (**Figure 4**). Together, our analyses support that hypokinetic symptoms
525 in PD are associated with reduced movement velocity and abnormal usage of behavioral
526 modules and that the therapeutic effects of L-DOPA are mediated by restoring velocities of
527 syllables but not their temporal organization.

528 Spontaneous movements have been closely linked with the slow changes in tonic DA
529 concentrations in the striatum [24]. Recent work demonstrates that SN DA neuronal activity and
530 the phasic striatal DA dynamics regulate movement initiation and generations of motor
531 sequences during spontaneous behavior [7,25,26]. Our observations from Parkinsonian mice are
532 largely consistent with these earlier reports. Specifically, the bradykinesia-like hypokinetic
533 motor deficits of mitoPark mice at the early motor stage with moderate striatal DA depletion

534 are mainly driven by the reduced velocities of faster behavioral modules. As the SN DA neurons
535 degenerate, the mitoPark mice gradually show decreases and increases in the usage of faster
536 and slower syllables, respectively, from the early motor stage at 14 weeks to the advanced
537 motor stage at 24 weeks (**Figures 2 and 3**). The combined effects of DA loss to syllable velocity
538 and usage lead to the manifestation of severely impaired locomotor activity in both models of
539 Parkinsonism.

540 Striatal DA transmission is critical in regulating goal-directed and spontaneous behavior
541 by modulating postsynaptic cellular function, synaptic transmission, and plasticity processes
542 within the corticostriatal circuits. Thus, the decreased velocity in Parkinsonism may be mainly
543 driven by the decreased tonic DA levels in the striatum and can be rescued by L-DOPA
544 administration. Moreover, we found that loss of DA downregulates the usage of several fast
545 syllables and upregulates the usage of several slow syllables in both 6-OHDA mice and late-stage
546 mitoPark mice. The altered usage of behavioral modules is likely to involve changes in striatal
547 DA dynamics (e.g., phasic DA release) or other maladaptive changes in the cortico-striatal
548 circuits that can't be rescued by acute L-DOPA administration.

549 Taking advantage of the progressive nature of mitoPark mice, we showed that behavior
550 modules with higher velocities (e.g., run- and walk-like syllables) were more vulnerable at early
551 stages than those involving whole-body coordination (e.g., turning and rearing). Moreover, the
552 magnitude of changes in the velocity and usage of the most vulnerable syllables increased from
553 the early to advanced stages of mitoPark mice. This might reflect the exaggerated damage of
554 cortico-basal ganglia circuits as the nigrostriatal pathway progressively degenerates. These data
555 suggest that distal limb control was probably affected earlier (e.g., at 14 weeks), leading to a

556 decreased expression of faster behavior modules at the early stages of nigrostriatal
557 degeneration. Subsequently, proximal limb control and whole-body coordination were impaired
558 at a later time point (e.g., 24 weeks), resulting in frequent pauses and fewer whole-body turns
559 during movements that might contribute to the development of freezing of gait-like behaviors
560 under parkinsonian state. Of relevance, the onset of motor symptoms in patients often starts
561 from the distal limbs (e.g., fingers and feet) [27], which might affect their performance in skilled
562 motor function or generate fast action sequences.

563 The literature on Parkinsonian animals has documented that nigrostriatal DA circuits are
564 required for generating stereotypical behavioral sequences [28]. The earlier studies focused on
565 species-specific behavioral sequences in rodents (e.g., grooming) because they are readily
566 identified by an experienced observer from recorded videos. Machine vision-based technologies
567 make it possible to expand this research to less visible behavioral sequences during natural
568 behavior. Using two mouse models of nigrostriatal degeneration, we documented that
569 degeneration of the nigrostriatal projections alters the usage of distinct behavioral modules and
570 decreases their transition probability in Parkinsonian states. This is consistent with earlier
571 studies documenting deficits in motion sequences and switches between motor programs in PD
572 patients [29].

573 Together, the progressive loss of DA does not alter behavioral modules in a
574 unidirectional, uniform, and all-at-once manner. This observation further indicates the
575 involvement of various biological mechanisms in regulating syllable velocity and usage and the
576 therapeutic efficacy of L-DOPA under Parkinsonian state, including the roles of tonic versus

577 phasic dopamine transmission by subtypes of nigral DA neurons [25], and potential contribution of
578 the motor cortical network [30].
579
580 PD is featured by progressive loss of nigrostriatal DA projections, starting from the
581 dopaminergic axons, followed by the loss of cell bodies [31]. This "dying back" pattern of
582 neurodegeneration has been recapitulated in several animal models, including the mitoPark
583 mice [8,32]. Thus, the compromised striatal DA levels in PD are expected to underlie the decreased
584 velocity and usage of fast behavioral modules in both mouse models of Parkinsonism in the
585 present study. L-DOPA administration can effectively restore tonic DA levels in the striatum,
586 which results in the rescued velocity of behavioral modules in Parkinsonian mice. This is
587 consistent with the observation that phasic DA transmission in the striatum does not modulate
588 movement kinematics [7,25]. Optogenetic stimulation of striatal dopaminergic axon terminals
589 induces rapid phasic transmission and increases the acceleration frequency, triggering the
590 initiation of locomotion. These observations indicate that phasic DA likely mediates the usages
591 of behavioral modules with fast velocities. Given that L-DOPA administration can't restore
592 phasic DA transmission, it explains the failure of L-DOPA in rescuing the usage of behavioral
593 modules in the late-stage mitoPark mice.
594 We demonstrated that L-DOPA rescued the decreased velocities of various behavior
595 syllables of Parkinsonian mitoPark mice but had little effect on the usage and transitions of
596 behavioral modules. Similar observations were reported by earlier studies in humans, showing
597 that levodopa improved the slowed movement but did not alleviate the sequence effects in PD
598 patients [33]. Acute L-DOPA may restore tonic dopamine levels in the striatum, which play a key

599 role in motor vigor and reinforcement learning [34]. L-DOPA-induced increases in the tonic striatal
600 DA levels likely underlie the restoration of motor velocity. Fast dopamine dynamics in the
601 striatum works as reinforcement to promote the use and organization of behavioral modules [7].
602 Thus, the disrupted behavioral sequencing in Parkinsonian mice is likely due to the impaired
603 phasic DA release in the striatum that systematic L-DOPA injections can't restore. However, we
604 can't exclude the involvement of other mechanisms, including maladaptive changes within and
605 outside the striatum, in the abnormal usage of behavioral modules and sequencing [35].
606 In conclusion, the present work reveals key features of behavioral module changes in
607 Parkinsonism. We demonstrated that loss of DA induces decreased velocity, abnormal usage,
608 and fewer transitions of behavioral modules during spontaneous behavior, underlying the
609 manifestation of hypokinetic deficits in PD. Further, we documented that acute L-DOPA-induced
610 therapeutic effects are largely mediated by its effects on the velocity of behavioral modules but
611 not their usages and sequences during spontaneous behavior. Further studies are warranted to
612 better understand the biological mechanisms underlying impaired behavioral sequencing after
613 loss of DA and design effective treatment to restore proper organization of naturalist behavior
614 in the Parkinsonian state.
615
616

Acknowledgement:

Behavior recordings were conducted at the Van Andel Research Institute. Data analysis and manuscript preparation were performed and completed at Georgetown University Medical Center. This work was partially supported by research grants from the National Institutes of Health (R01NS121371, R21NS135545, H.Y.C; and R01NS133338, S.M.D. and H.Y.C.), Department of Defense Congressionally Directed Medical Research Programs (W81XWH-21-1-0943, H.Y.C.), and Parkinson's Foundation (PF-IMP-1045313, H.Y.C.). This work was also funded in whole or in part by Aligning Science Across Parkinson's (ASAP-020572) through the Michael J. Fox Foundation for Parkinson's Research (MJFF). For the purpose of open access, the authors have applied a CC BY public copyright license to all Author Accepted Manuscripts arising from this submission.

Author contributions:

Conceptualization (DB, HYC); Investigation (DB, GS, HDC, LC); Formal analysis (DB, HYC); Validation (DB, LC, HYC); Writing – original draft (DB, HYC); Writing – Review & Editing (HYC); Supervision, Project administration and Funding acquisition (HYC).

Authors' ORCID:

Daniil Berezhnoi: 0000-0001-7507-0589

Hiba Douja Chehade: 0000-0002-5959-7900

Liqiang Chen: 0000-0003-3236-1129

Hong-Yuan Chu: 0000-0003-0923-683X

Availability of data and materials. The raw and analyzed during the current study have been deposited and are publicly available from Github (https://github.com/ChuLab-GU/behavior-analysis) and Zenodo (https://zenodo.org/records/14555868).

Competing interests. The authors declare that they have no competing interests.

References cited

1. Obeso, J.A., Stamelou, M., Goetz, C.G., Poewe, W., Lang, A.E., Weintraub, D., Burn, D., Halliday, G.M., Bezard, E., Przedborski, S., et al. (2017). Past, present, and future of Parkinson's disease: A special essay on the 200th Anniversary of the Shaking Palsy. Movement Disorders *32*, 1264-1310. 10.1002/mds.27115.
2. Goetz, C.G., Tilley, B.C., Shaftman, S.R., Stebbins, G.T., Fahn, S., Martinez-Martin, P., Poewe, W., Sampaio, C., Stern, M.B., Dodel, R., et al. (2008). Movement Disorder Society-sponsored revision of the Unified Parkinson's Disease Rating Scale (MDS-UPDRS): scale presentation and clinimetric testing results. Mov Disord *23*, 2129-2170. 10.1002/mds.22340.
3. Gschwind, T., Zeine, A., Raikov, I., Markowitz, J.E., Gillis, W.F., Felong, S., Isom, L.L., Datta, S.R., and Soltesz, I. (2023). Hidden behavioral fingerprints in epilepsy. Neuron *111*, 1440-1452 e1445. 10.1016/j.neuron.2023.02.003.
4. Miller, S.R., Luxem, K., Lauderdale, K., Nambiar, P., Honma, P.S., Ly, K.K., Bangera, S., Bullock, M., Shin, J., Kaliss, N., et al. (2024). Machine learning reveals prominent spontaneous behavioral changes and treatment efficacy in humanized and transgenic Alzheimer's disease models. Cell Rep *43*, 114870. 10.1016/j.celrep.2024.114870.
5. Wiltschko, Alexander B., Johnson, Matthew J., Iurilli, G., Peterson, Ralph E., Katon, Jesse M., Pashkovski, Stan L., Abraira, Victoria E., Adams, Ryan P., and Datta, Sandeep R. (2015). Mapping Sub-Second Structure in Mouse Behavior. Neuron *88*, 1121-1135. 10.1016/j.neuron.2015.11.031.
6. Markowitz, J.E., Gillis, W.F., Beron, C.C., Neufeld, S.Q., Robertson, K., Bhagat, N.D., Peterson, R.E., Peterson, E., Hyun, M., Linderman, S.W., et al. (2018). The Striatum Organizes 3D Behavior via Moment-to-Moment Action Selection. Cell *174*, 44-58.e17. 10.1016/j.cell.2018.04.019.
7. Markowitz, J.E., Gillis, W.F., Jay, M., Wood, J., Harris, R.W., Cieszkowski, R., Scott, R., Brann, D., Koveal, D., Kula, T., et al. (2023). Spontaneous behaviour is structured by reinforcement without explicit reward. Nature *614*, 108-117. 10.1038/s41586-022-05611-2.
8. Ekstrand, M.I., Terzioglu, M., Galter, D., Zhu, S., Hofstetter, C., Lindqvist, E., Thams, S., Bergstrand, A., Hansson, F.S., Trifunovic, A., et al. (2007). Progressive parkinsonism in mice with respiratory-chain-deficient dopamine neurons. Proceedings of the National Academy of Sciences *104*, 1325-1330. 10.1073/pnas.0605208103.
9. Galter, D., Pernold, K., Yoshitake, T., Lindqvist, E., Hoffer, B., Kehr, J., Larsson, N.G., and Olson, L. (2010). MitoPark mice mirror the slow progression of key symptoms and L-DOPA response in Parkinson's disease. Genes Brain Behav *9*, 173-181. 10.1111/j.1601-183x.2009.00542.x.
10. Beckstead, M.J., and Howell, R.D. (2021). Progressive parkinsonism due to mitochondrial impairment: Lessons from the MitoPark mouse model. Exp Neurol *341*, 113707. 10.1016/j.expneurol.2021.113707.
11. Ekstrand, M.I., and Galter, D. (2009). The MitoPark Mouse – An animal model of Parkinson's disease with impaired respiratory chain function in dopamine neurons. Parkinsonism & Related Disorders *15*, S185-S188. 10.1016/s1353-8020(09)70811-9.

12. Weinreb, C., Pearl, J.E., Lin, S., Osman, M.A.M., Zhang, L., Annapragada, S., Conlin, E., Hoffmann, R., Makowska, S., Gillis, W.F., et al. (2024). Keypoint-MoSeq: parsing behavior by linking point tracking to pose dynamics. Nat Methods *21*, 1329-1339. 10.1038/s41592-024-02318-2.
13. Gawande, D.Y., KK, S.N., Shelkar, G.P., Pavuluri, R., Stessman, H.A.F., and Dravid, S.M. (2023). GluN2D Subunit in Parvalbumin Interneurons Regulates Prefrontal Cortex Feedforward Inhibitory Circuit and Molecular Networks Relevant to Schizophrenia. Biol Psychiatry *94*, 297-309. 10.1016/j.biopsych.2023.03.020.
14. Vila, M., Perier, C., Feger, J., Yelnik, J., Faucheux, B., Ruberg, M., Raisman-Vozari, R., Agid, Y., and Hirsch, E.C. (2000). Evolution of changes in neuronal activity in the subthalamic nucleus of rats with unilateral lesion of the substantia nigra assessed by metabolic and electrophysiological measurements. Eur J Neurosci *12*, 337-344. 10.1046/j.1460-9568.2000.00901.x.
15. Chen, L., Daniels, S., Kim, Y., and Chu, H.-Y. (2021). Cell Type-Specific Decrease of the Intrinsic Excitability of Motor Cortical Pyramidal Neurons in Parkinsonism. J Neurosci *41*, 5553-5565. 10.1523/jneurosci.2694-20.2021.
16. Masini, D., Plewnia, C., Bertho, M., Scalbert, N., Caggiano, V., and Fisone, G. (2021). A Guide to the Generation of a 6-Hydroxydopamine Mouse Model of Parkinson's Disease for the Study of Non-Motor Symptoms. Biomed *9*, 598. 10.3390/biomedicines9060598.
17. Chen, L., Daniels, S., Dvorak, R., and Chu, H.Y. (2023). Reduced thalamic excitation to motor cortical pyramidal tract neurons in parkinsonism. Sci Adv *9*, eadg3038. 10.1126/sciadv.adg3038.
18. Mallet, N., Pogosyan, A., Sharott, A., Csicsvari, J., Bolam, J.P., Brown, P., and Magill, P.J. (2008). Disrupted dopamine transmission and the emergence of exaggerated beta oscillations in subthalamic nucleus and cerebral cortex. J Neurosci Official J Soc Neurosci *28*, 4795-4806. 10.1523/JNEUROSCI.0123-08.2008.
19. Chu, H.Y. (2020). Synaptic and cellular plasticity in Parkinson's disease. Acta Pharmacol Sin *41*, 447-452. 10.1038/s41401-020-0371-0.
20. Chu, H.-Y., McIver, E.L., Kovaleski, R.F., Atherton, J.F., and Bevan, M.D. (2017). Loss of hyperdirect pathway cortico-subthalamic inputs following degeneration of midbrain dopamine neurons. Neuron *95*, 1306-1318.e1305. 10.1016/j.neuron.2017.08.038.
21. Wiltschko, A.B., Tsukahara, T., Zeine, A., Anyoha, R., Gillis, W.F., Markowitz, J.E., Peterson, R.E., Katon, J., Johnson, M.J., and Datta, S.R. (2020). Revealing the structure of pharmacobehavioral space through motion sequencing. Nat Neurosci *23*, 1433-1443. 10.1038/s41593-020-00706-3.
22. Panigrahi, B., Martin, Kathleen A., Li, Y., Graves, Austin R., Vollmer, A., Olson, L., Mensh, Brett D., Karpova, Alla Y., and Dudman, Joshua T. (2015). Dopamine Is Required for the Neural Representation and Control of Movement Vigor. Cell *162*, 1418-1430. 10.1016/j.cell.2015.08.014.
23. Yttri, E.A., and Dudman, J.T. (2016). Opponent and bidirectional control of movement velocity in the basal ganglia. Nature *533*, 402-406. 10.1038/nature17639.
24. Schultz, W. (2007). Multiple dopamine functions at different time courses. Annu Rev Neurosci *30*, 259-288. 10.1146/annurev.neuro.28.061604.135722.

25. Howe, M.W., and Dombeck, D.A. (2016). Rapid signalling in distinct dopaminergic axons during locomotion and reward. Nature *535*, 505-510. 10.1038/nature18942.
26. da Silva, J.A., Tecuapetla, F., Paixao, V., and Costa, R.M. (2018). Dopamine neuron activity before action initiation gates and invigorates future movements. Nature *554*, 244-248. 10.1038/nature25457.
27. Monje, M.H.G., Sanchez-Ferro, A., Pineda-Pardo, J.A., Vela-Desojo, L., Alonso-Frech, F., and Obeso, J.A. (2021). Motor Onset Topography and Progression in Parkinson's Disease: the Upper Limb Is First. Mov Disord *36*, 905-915. 10.1002/mds.28462.
28. Berridge, K.C. (1989). Substantia nigra 6-OHDA lesions mimic striatopallidal disruption of syntactic grooming chains: A neural systems analysis of sequence control. Psychobiology *17*, 377-385. 10.3758/BF03337797.
29. Benecke, R., Rothwell, J.C., Dick, J.P., Day, B.L., and Marsden, C.D. (1987). Disturbance of sequential movements in patients with Parkinson's disease. Brain *110 (Pt 2)*, 361-379. 10.1093/brain/110.2.361.
30. Nicholas, M.A., and Yttri, E.A. (2024). Motor cortex is responsible for motoric dynamics in striatum and the execution of both skilled and unskilled actions. Neuron *112*, 3486-3501 e3485. 10.1016/j.neuron.2024.07.022.
31. Chu, Y., Morfini, G.A., Langhamer, L.B., He, Y., Brady, S.T., and Kordower, J.H. (2012). Alterations in axonal transport motor proteins in sporadic and experimental Parkinson's disease. Brain *135*, 2058-2073. 10.1093/brain/aws133.
32. Good, C.H., Hoffman, A.F., Hoffer, B.J., Chefer, V.I., Shippenberg, T.S., Bäckman, C.M., Larsson, N.-G., Olson, L., Gellhaar, S., Galter, D., and Lupica, C.R. (2011). Impaired nigrostriatal function precedes behavioral deficits in a genetic mitochondrial model of Parkinson's disease. Faseb J *25*, 1333-1344. 10.1096/fj.10-173625.
33. Kang, S.Y., Wasaka, T., Shamim, E.A., Auh, S., Ueki, Y., Lopez, G.J., Kida, T., Jin, S.H., Dang, N., and Hallett, M. (2010). Characteristics of the sequence effect in Parkinson's disease. Mov Disord *25*, 2148-2155. 10.1002/mds.23251.
34. Niv, Y., Daw, N.D., Joel, D., and Dayan, P. (2007). Tonic dopamine: opportunity costs and the control of response vigor. Psychopharmacology (Berl) *191*, 507-520. 10.1007/s00213-006-0502-4.
35. Gonzalez-Rodriguez, P., Zampese, E., Stout, K.A., Guzman, J.N., Ilijic, E., Yang, B., Tkatch, T., Stavarache, M.A., Wokosin, D.L., Gao, L., et al. (2021). Disruption of mitochondrial complex I induces progressive parkinsonism. Nature *599*, 650-656. 10.1038/s41586-021-04059-0.

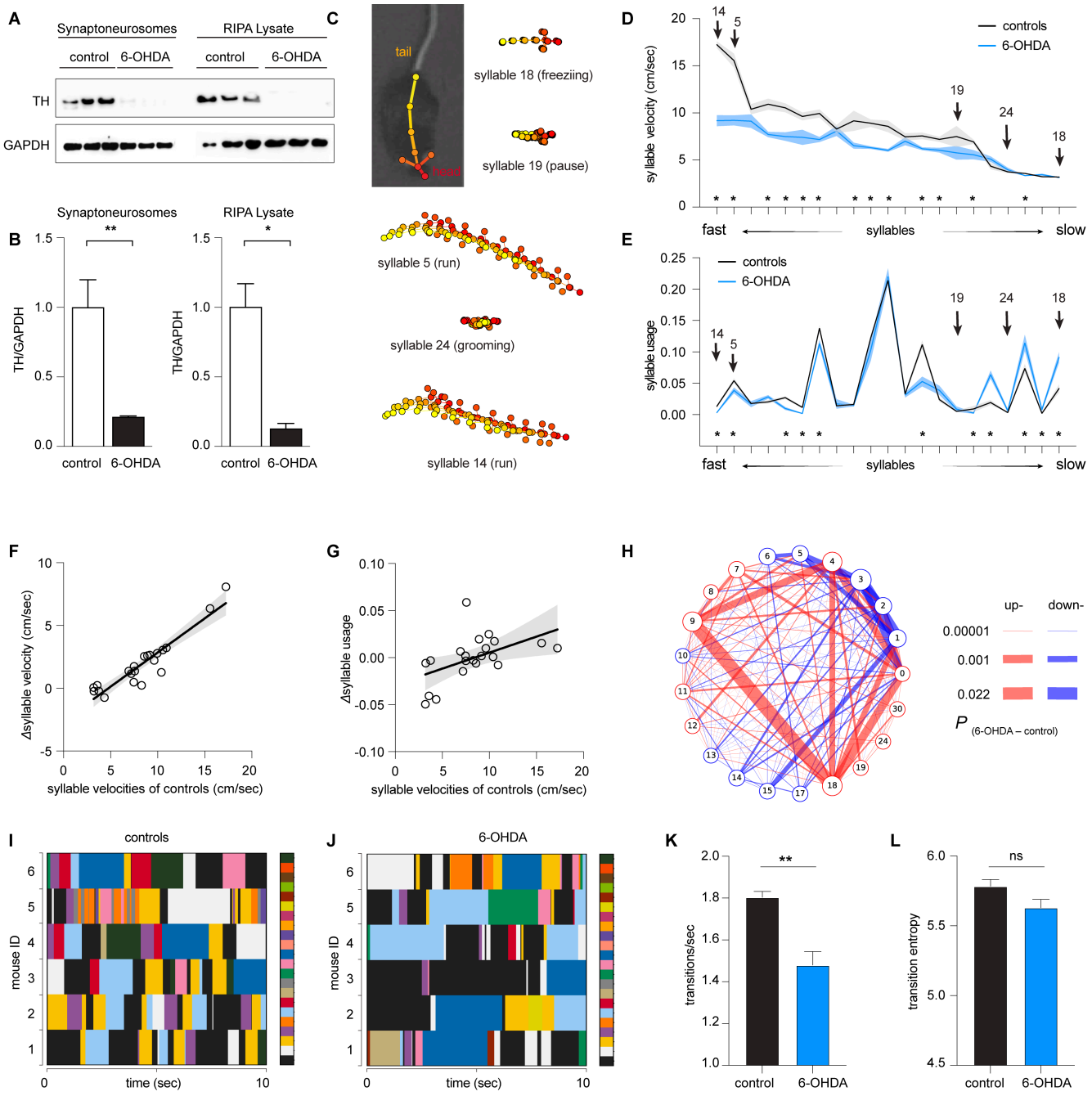
A
Synaptoneurosomes
RIPA Lysate
control
6-OHDA
control
6-OHDA
TH
GAPDH
B
Synaptoneurosomes
RIPA Lysate
**
*
TH/GAPDH
control
6-OHDA
C
tail
head
syllable 18 (freeziing)
syllable 19 (pause)
syllable 5 (run)
syllable 24 (grooming)
syllable 14 (run)
D
controls
6-OHDA
syllable velocity (cm/sec)
fast
syllables
slow
E
controls
6-OHDA
syllable usage
fast
syllables
slow
F
Δsyllable velocity (cm/sec)
syllable velocities of controls (cm/sec)
G
Δsyllable usage
syllable velocities of controls (cm/sec)
H
up-
down-
0.00001
0.001
0.022
P (6-OHDA – control)
I
controls
mouse ID
time (sec)
J
6-OHDA
mouse ID
time (sec)
K
**
transitions/sec
control
6-OHDA
L
ns
transition entropy
control
6-OHDA

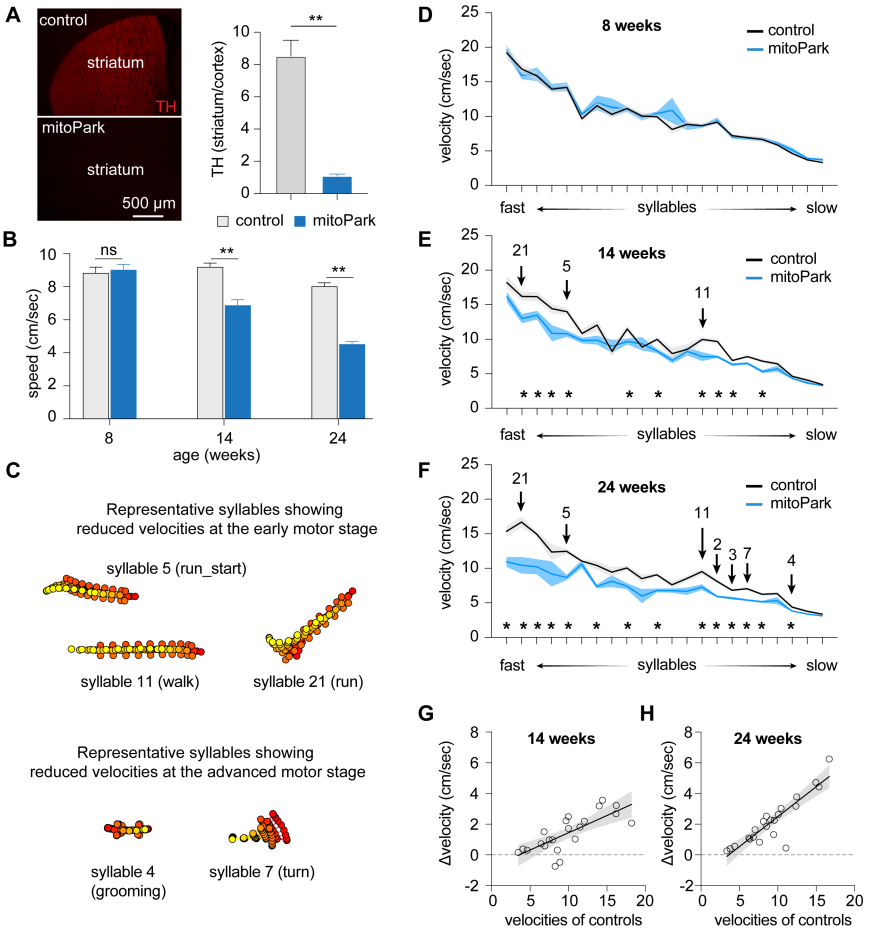
A
control
striatum
TH
mitoPark
striatum
500 µm
TH (striatum/cortex)
**
control
mitoPark
B
speed (cm/sec)
ns
**
**
8
14
24
age (weeks)
C
Representative syllables showing
reduced velocities at the early motor stage
syllable 5 (run_start)
syllable 11 (walk)
syllable 21 (run)
Representative syllables showing
reduced velocities at the advanced motor stage
syllable 4
(grooming)
syllable 7 (turn)
D
8 weeks
control
mitoPark
velocity (cm/sec)
fast
syllables
slow
E
14 weeks
21
5
11
F
24 weeks
2
3
7
4
G
14 weeks
Δvelocity (cm/sec)
velocities of controls
H
24 weeks

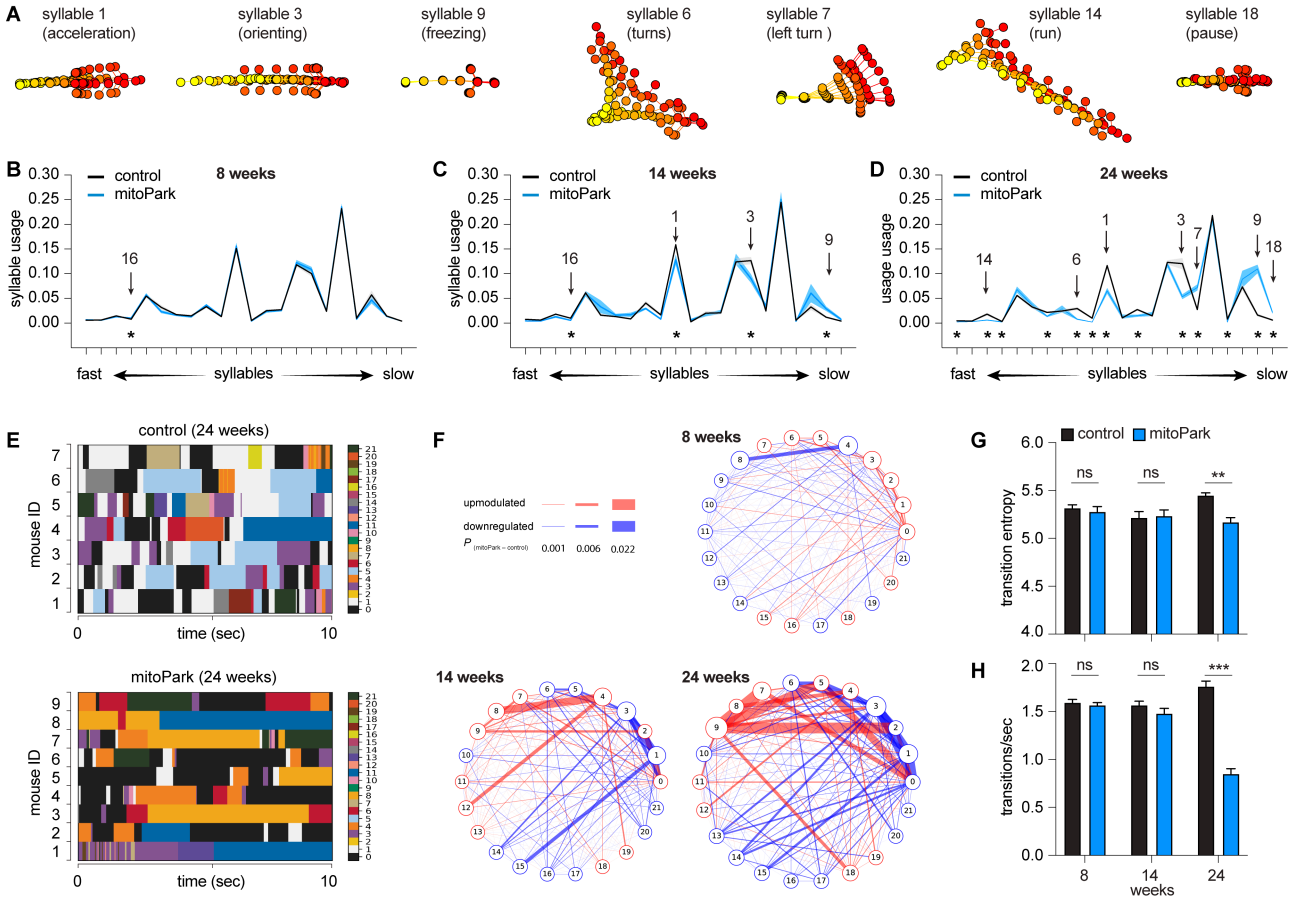
A
syllable 1 (acceleration)
syllable 3 (orienting)
syllable 9 (freezing)
syllable 6 (turns)
syllable 7 (left turn)
syllable 14 (run)
syllable 18 (pause)
B
8 weeks
control
mitoPark
syllable usage
fast
syllables
slow
C
14 weeks
D
24 weeks
usage usage
E
control (24 weeks)
mitoPark (24 weeks)
mouse ID
time (sec)
F
upmodulated
downregulated
8 weeks
14 weeks
24 weeks
G
transition entropy
ns
**
H
transitions/sec
***
weeks

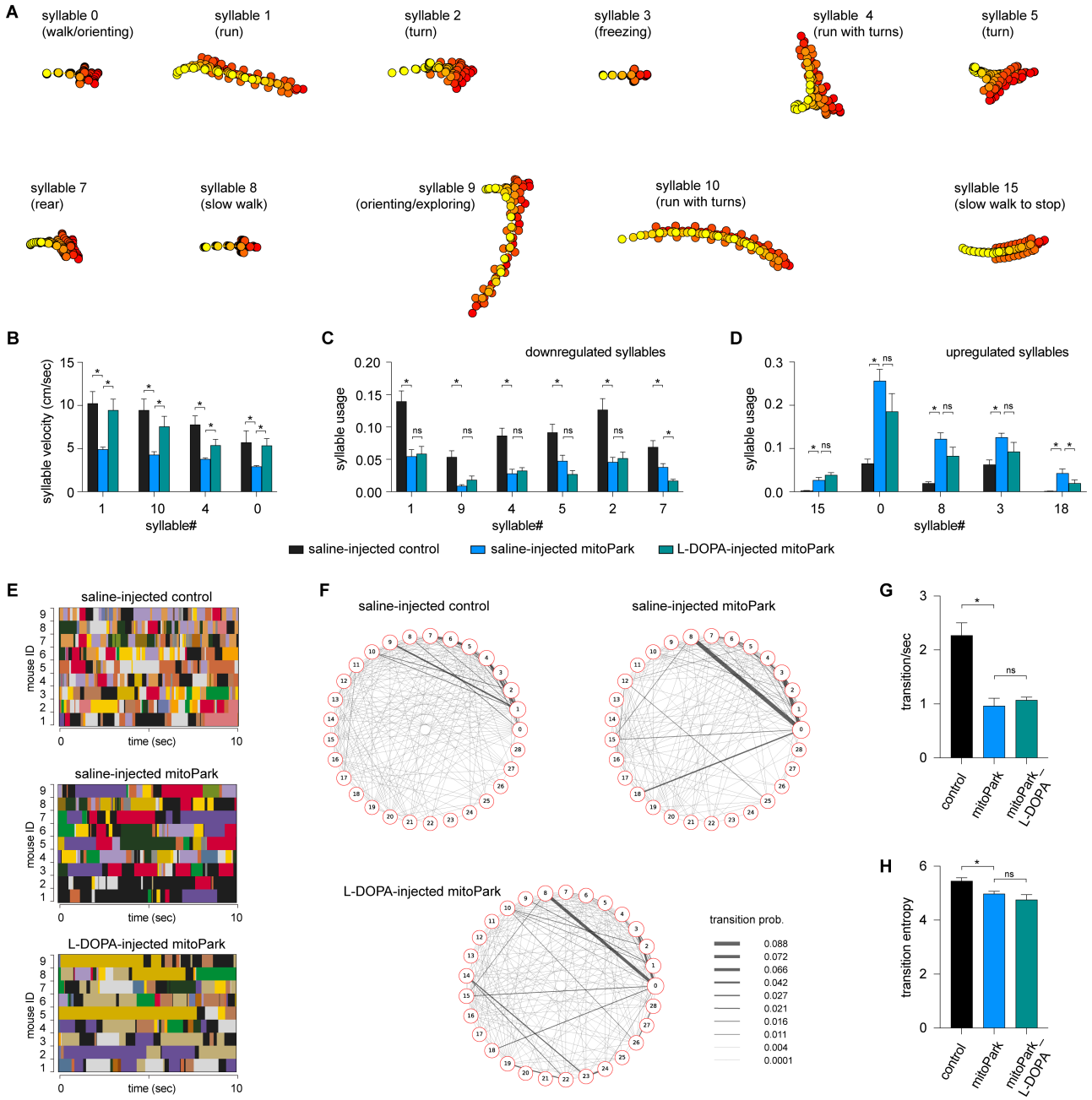
A
syllable 0 (walk/orienting)
syllable 1 (run)
syllable 2 (turn)
syllable 3 (freezing)
syllable 4 (run with turns)
syllable 5 (turn)
syllable 7 (rear)
syllable 8 (slow walk)
syllable 9 (orienting/exploring)
syllable 10 (run with turns)
syllable 15 (slow walk to stop)
B
syllable velocity (cm/sec)
syllable#
C
downregulated syllables
syllable usage
syllable#
D
upregulated syllables
syllable usage
syllable#
saline-injected control
saline-injected mitoPark
L-DOPA-injected mitoPark
E
saline-injected control
saline-injected mitoPark
L-DOPA-injected mitoPark
mouse ID
time (sec)
F
saline-injected control
saline-injected mitoPark
L-DOPA-injected mitoPark
transition prob.
0.088
0.072
0.066
0.042
0.027
0.021
0.016
0.011
0.004
0.0001
G
transition/sec
control
mitoPark
mitoPark_L-DOPA
H
transition entropy
control
mitoPark
mitoPark_L-DOPA